Preliminary Results From Herschel-SPIRE Flight Instrument Testing

Tanya Lim[a], Bruce Swinyard[a], Matthew Griffin[b], Asier Aramburu[a], Jean-Paul Baluteau[c], James Bock[d], Marc Ferlet[a], Trevor Fulton[e], Douglas Griffin[a], Steven Guest[a], Peter Hargrave[b], Kenneth King[a], Sarah Leeks[f], David Naylor[e], Edward Polehampton[a], Davide Rizzo[g], Eric Sawyer[a], Bernhard Schulz[h], Sunil Sidher[a], Locke Spencer[e], David Smith[a], Hien Trong Nguen[d], Ivan Valtchanov[f], Tim Waskett[b], Adam Woodcraft[b]

a Rutherford Appleton Laboratory, CCLRC, Chilton, Didcot, Oxon, OX11 OQX, UK
b Cardiff University, School of Physics and Astronomy, 5 The Parade, Cardiff CF24 3YB, UK
c Laboratoire d'Astrophysique Marseille, CNRS & Université de Provence, BP 8, 13376 Marseille Cedex 12, France
d Jet Propulsion Laboratory, 4800 Oak Grove Drive, Pasadena, CA 91109, USA
e University of Lethbridge, Department of Physics, Lethbridge, Alberta T1K 3M4, Canada
f Astrophysics Missions Division of ESA, ESTEC, Keplerlaan 1, 2200 AG Noordwijk, NL
g Imperial College of Science, Technology and Medicine, Blackett Laboratory, Exhibition Road, London SW7 2AZ
h Infrared Processing and Analysis Center, California Institute of Technology, Pasadena, CA 91125, USA

ABSTRACT

The Spectral and Photometric Imaging REceiver (SPIRE) is one of the three scientific instruments to fly on the European Space Agency's Herschel Space Observatory, and contains a three-band imaging submillimetre photometer and an imaging Fourier transform spectrometer. The flight model of the SPIRE cold focal plane unit has been built up in stages with a cold test campaign associated with each stage. The first campaign focusing on the spectrometer took place in early 2005 and the second campaign focusing on the photometer was in Autumn 2005. SPIRE is currently undergoing its third cold test campaign following cryogenic vibration testing. Test results to date show that the instrument is performing very well and in general meets not only its requirements but also most of its performance goals. We present an overview of the instrument tests performed to date, and the preliminary results.

Keywords: Herschel, Far Infrared, Submillimetre, Bolometer, Instrumentation

1. INTRODUCTION

The Spectral and Photometric Imaging Receiver (SPIRE)[1] is one of three instruments to fly on the European Space Agency's Herschel Space Observatory[2], and is designed for direct detection observations in the 200-700 μm range. It consists of a cold focal plane unit (FPU), which will be mounted on the 10-K instrument optical bench inside the Herschel cryostat, and a set of warm electronics units located some distance away on the Herschel service module. The FPU enclosure will be vapour-cooled to approximately 4.5 K, by the boil-off from the Herschel helium tank, and cooling to 1.7 K for some internal elements will also be provided via direct thermal strap to the helium tank The FPU comprises a three-band imaging photometer with bands centred at approximately 250, 360 and 520 μm, and an imaging Fourier Transform Spectrometer (FTS) covering 200-670 μm. The detectors for both sub-instruments are feedhorn-coupled NTD spider-web bolometers[3] cooled to 300 mK by a closed cycle ^{3}He refrigerator. The refrigerator has a recycle cycle time of less than two hours and a predicted hold time of more than 46 hours. The bolometer signals are conditioned using JFET pre-amplifiers operating at ~ 120 K, situated close to the FPU and connected to the readout electronics via a 7-m long harness. There is no signal multiplexing at the cold end of the system - each bolometer is read

out differentially using sinusoidal bias and individual lock-in amplifiers.

The photometer and spectrometer fields of view are spatially separated and the two sub-instruments do not operate simultaneously. The photometer has a rectangular field of view of 4 x 8 arcmin. and the spectrometer a circular field of view of 2.6 arcmin. The photometer field of view is observed simultaneously in the three spectral bands using two cascaded dichroic beamsplitters, with angular resolution determined in all three bands by the telescope diffraction limit. The FWHM beam widths will be approximately 17, 24 and 35" at 250, 360 and 520 μm respectively. An internal beam steering mirror allows spatial modulation of the telescope beam for both photometer and spectrometer. Mapping observations can also be made by scanning the telescope. The spectrometer uses a dual-beam (Mach-Zehnder) configuration with broad-band intensity beam dividers. The FTS scanning mirror has a linear travel of up to 3.5 cm, which, with an optical folding factor of four, provides adjustable spectral resolution from 0.04 – 2 cm^{-1} ($\lambda/\Delta\lambda$ = 20 - 1000 at 250 μm).

Internal thermal calibration sources are installed in both the photometer and spectrometer sub-instruments. The photometer calibrator (Pcal) is used to provide a repeatable signal for the bolometers. It radiates through a hole in the centre of the beam steering mirror, occupying an area contained within the region of the pupil obscured by the hole in the primary. The source can produce a power at the detector of 1-2% of the telescope background, giving a large instantaneous S/N at the detectors. It is foreseen that it will be operated for a few seconds at intervals of several tens of minutes, in order to track any variations in detector responsivity. The spectrometer calibration source (Scal) serves a different purpose. It is located at the second input port of the FTS, and is designed to null the central maximum of the interferogram by radiating the same amount of power onto the detectors as they receive from the telescope. It consists of two adjustable-temperature black body emitters, one of which fills approximately 4% of the pupil area and the other approximately 2%. They can be operated separately or together to null the intensity and the spectrum of the telescope as effectively as possible.

The SPIRE FPU development programme has consisted of several builds. The SPIRE cryogenic qualification model (CQM) was the first instrument model built to undergo performance testing. The cold focal plane unit comprised a combination of flight-like components and mass dummies and was been built to serve two main purposes: to allow the optical, thermal, and electronic systems to be operated in as close to flight conditions as possible so that any major problems in the design could be identified ahead of the flight instrument, and to allow a representative cryogenic vibration test to be done on a working instrument, again to allow any major design flaws to be identified before committing to the flight instrument. For cost and schedule reasons, the FPU was not fully equipped with all of the subsystems. It contained a single channel of the photometer (the 520-μm band) with an engineering-grade bolometer array cooled by a fully representative ^{3}He refrigerator. The bolometer signals were conditioned by a single 48-channel JFET amplifier module with seven other JFET modules replaced by dummy resistor networks to provide a passive but representative load to the warm lock-in amplifiers. The full set of instrument optics, filters, and dichroics was fitted as the pass-band is controlled by the combination of all the filters within the SPIRE instrument. The beam steering mirror was replaced by a mass thermal dummy as were the other four detector arrays and the spectrometer scan mechanism. Results from the CQM testing are described in Lim e*t al.* [3]

The first build of the proto-flight model (FM) FPU contained the complete spectrometer side of the instrument with flight subsystems except for the spectrometer mechanism, for which a scientifically representative qualification model was installed. The first cold test campaign took place in spring 2005 and was aimed at assessing the spectrometer performance. The instrument was then upgraded to include the flight photometer arrays and a second flight model (PFM2) test campaign took place in autumn 2005. Although all arrays were present, not all LIAs were yet equipped in the warm electronics used, and only around half the pixels were active. This campaign focussed on assessing the performance of the photometer.

The FPU then underwent a qualification level cold vibration test. At the time of writing, a post-vibration performance test campaign has started. The installation of the flight spectrometer mechanism is planned to take place in June 2006 after which the FPU will undergo a final cold vibration followed by an extended calibration campaign in autumn 2006 before delivery to ESA.

In this paper we report on the tests carried out so far during the performance testing of the instrument, and present some of the results of those tests. In the next section we describe the test facility used and give an outline of the test programme and the remaining sections then describe the main results from the tests.

2. THE SPIRE INSTRUMENT TEST FACILITY

The cryogenic test facility[4] has two working areas (Fig. 1): a clean room housing the custom-built SPIRE test cryostat and optical benches, and a control room housing the instrument Electronic Ground Support Equipment (EGSE) and Test Facility Control System (TFCS). The clean room is at class 10,000 except in the area of the cryostat where the class is 1000. The cryostat (Fig. 2) simulates the in-flight thermal conditions provided by the Herschel cryostat with temperature stages of 10 K, 4.2 K and 1.7 K. The instrument can view a room-temperature telescope simulator via a PTFE window on the cryostat vacuum vessel. A set of thermal filters on the liquid nitrogen cooled cryostat shield and the helium gas-cooled "10-K" shield remove most of the thermal infrared from the ambient room background. A pair of neutral density filters placed on the 4.2-K shield reduces the in-band radiant background to a level equivalent to that expected from the 80-K, 4% emissive Herschel telescope. A cryogenic black body source is also provided inside the cryostat. This can be viewed directly by the instrument via a flip mirror, and completely fills the instrument field of view. When the cryogenic black body is unheated it is used as the dark reference for the instrument, and when it is heated it can reach up to 40 K in a few tens of minutes. The hold time of the cryostat is more than 24 hours.

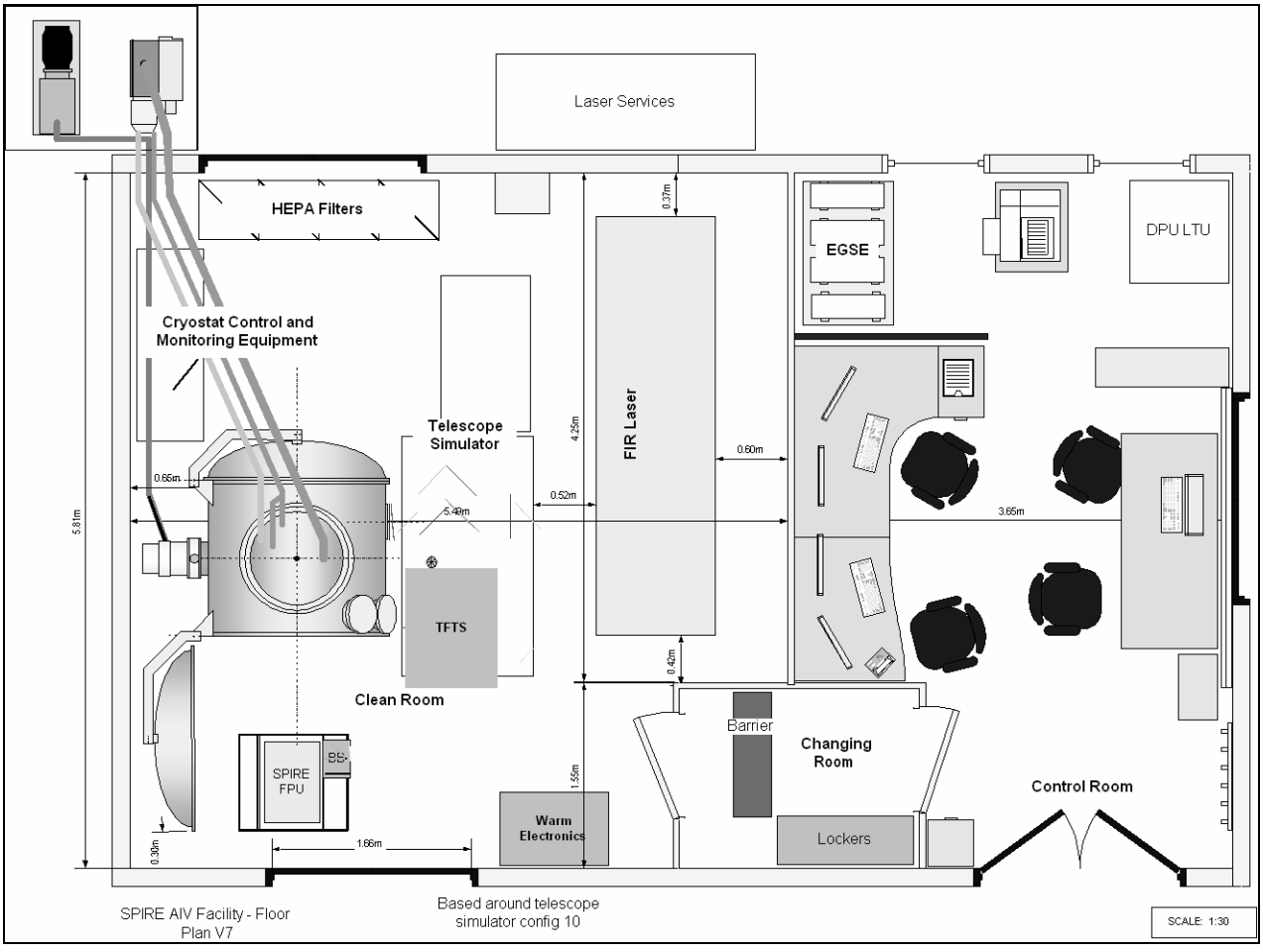

Figure 1: Layout of the SPIRE test facility.

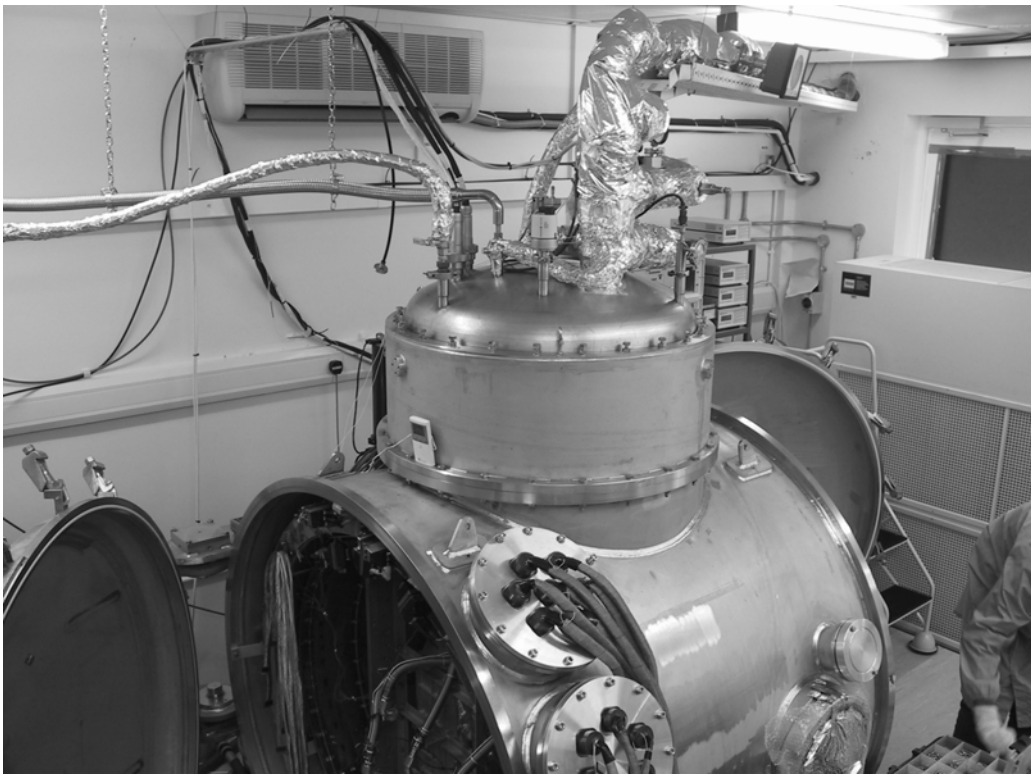

Figure 2: Photograph of the SPIRE test cryostat

Two external sources, a hot black body and a far infrared/submillimetre laser, can be coupled to SPIRE via a room-temperature telescope simulator situated on a low level optical bench next to the cryostat. The telescope simulator presents the instrument with an *f*/8.68 beam via a pupil mask which correctly represents the input from the Herschel telescope. Two fold mirrors within the simulator optical train can be scanned to place a source at the input of the telescope simulator anywhere within the SPIRE field of view.

The adjustable-temperature black body source is used as the input source to a test FTS[5] (TFTS), the output of which is coupled to the input of the telescope simulator. The TFTS provides a spectral scan of the black body allowing measurement of the photometer spectral response. With the FTS mirrors stationary, the same black body provides a point source which can be scanned over the SPIRE field of view. The telescope simulator and TFTS are situated in a dry air enclosure allowing operation in relative humidity as low as 6-10%. The optical configuration can be manually changed to place the blackbody in the telescope simulator pupil plane and the two scanning mirrors can then be used to scan the point source laterally to measure the illumination pattern with which the SPIRE detector feedhorns will illuminate the secondary mirror of the Herschel telescope.

The far infrared laser is an Edinburgh Instruments model PL295 gas laser, pumped by a CO_2 laser equipped with an active stabilisation system to ensure constant laser power output. The laser gives a range of lines from 10.6 μm to 2 mm and there are numerous lines covering the SPIRE band.

3. OVERVIEW OF THE TEST PROGRAMME

Performance tests are divided into three basic types:

(i) thermal balance tests, during which the basic thermal design of the instrument is evaluated;
(ii) "closed" cryostat testing with the instrument viewing the internal cryogenic black body to provide low-background conditions representative of the flight environment;
(iii) optical testing with the instrument viewing the external telescope simulator via the cryostat entrance window.

3.1 Thermal balance tests

The most basic thermal tests involved verifying that the different temperature stages of both the cryostat and the instrument achieved the required temperatures. All temperatures were as expected during testing. Operation of the ^{3}He cooler is nominal, with operational temperature (approx. 285 mK) achieved within two hours of the start of cooler recycle. The cooler has also met performance requirements with the nominal 1.7 K interface temperature, operating for over 48 hours with the full flight instrument.

3.2 Closed cryostat tests

One of the most important objectives of the test programme so far has been to demonstrate that the integrated system (FPU + harness + warm electronics) will function correctly and that no excess noise is introduced due to ground loops, electromagnetic interference, bias supply noise, microphonics, etc. Detector noise measurements were carried out on the detectors under minimum photon background conditions, and V-I characteristics (load curves) have been measured under a number of different bias and optical loading conditions, using the cryogenic black body to set the photon background. From these measurements it has been possible to determine the operating temperatures of the bolometers and relate these to the absorbed power levels. The results of the noise and load curve measurements are reported in Section 4.

3.3 Optical tests

The external source and the telescope simulator were used to measure the centre positions of several pixels and to characterise in detail the beam profile on the sky of the central detector. The TFTS was used to measure the spectral passband for the same set of pixels. The external source was also used to illuminate the pupil to measure the conjugate beam response of a single pixel. Finally, the laser was used to illuminate the array to search for stray light glints and to verify the frequency response of the detectors using a variable frequency chopper. We report on the optical test results in Section 5.

The performances of the mechanisms and the internal calibrators have also assessed under various representative conditions. In Section 6 the calibrators performance is discussed then in sections 7 and 8 the performance of the beam steering mechanism and the spectrometer mechanism (SMEC) are discussed.

4. CLOSED CRYOSTAT TESTING

4.1 Load curves

Load curves (measurements of the bolometer voltage as a function of current) enable the parameters describing the electrical and thermal properties of a semiconductor bolometer to be determined. The performance of the bolometer can then be reliably predicted for different operating conditions. Excellent agreement has been found between load curves measured in the SPIRE FPU and those measured during unit-level testing of the bolometer arrays at JPL. Load curve

measurements also allow the absorbed power to be estimated, enabling the overall photometric throughput of the instrument to be determined from load curves taken with the instrument viewing a calibrated cryogenic black body (see Section 4.3). The overall channel yield (taking into account the complete chain of bolometer, JFET, cryoharness LIA) is very good and is far higher than the requirement of 80%.

4.2 Detector noise

The detector noise was measured through the complete system under three different conditions:

(i) with the bolometers at a temperature of > 1.7 K, and therefore of very low impedance - this measured the input-short noise of the complete electronics chain (JFETs, cryo-harness, and warm electronics) in isolation and allowed a characterisation of noise versus the JFET operating voltage;

(ii) with the bolometers at nominal operating temperature and bias and with minimum photon background, during long (overnight) test periods – this allowed the baseline note level and stability to be evaluated;

(iii) with the detectors under a range of bias levels, with nominal temperature, and both nominal and minimum photon background - this measured the complete system noise.

Data from all five detector arrays were analysed, although not all channels were operational due to missing LIA channels and some harness disconnects. The large majority of channels signals show only 10-30% more noise respectively than the theoretical expectations from model calculations made for the actual bolometer parameters and biases that were used. Some thermal instability problems were apparent, and are though to be associated with the operational environment of the instrument. These will be investigated further in future cooldowns.

4.3 Instrument optical efficiency

Using load curves taken with the instrument viewing the cold black body at two different temperatures (6.4 K and at 13 K) the temperature rise in the bolometers was measured and the absorbed power in the detectors calculated using established bolometer theory[6] and the detector parameters previously determined at unit level. The results were compared with the predictions of a photometric model with the parameters outlined in Table 1, integrating over the black body function to derive the expected absorbed power. The ratio of the measured and expected powers should be unity if there are no unaccounted losses in the instrument. Typical results, for the 520 μm photometer array, are shown in Figure 3.

Parameter	Derived from	Value
Instrument spectral passband	Measurements of individual filters and feedhorn specification	See section 5.1
Detector-feedhorn optical efficiency	Derived in unit level tests	Varies with detector type
Optical throughput ($A\Omega$)	Theoretical expected for a single mode	λ^2
Expected cold stop efficiency	Optical model	0.84
Loss due to the hole in the BSM for the calibration source	Metrology	0.95
Loss due to absorption and scattering from mirrors	Estimate	0.99 per mirror
Cold black body temperatures	Measured thermometry	6.4 K and 13 K
Cold black body emissivity	Estimate	1.00

Table 1: Model parameters used to derive the optical efficiency

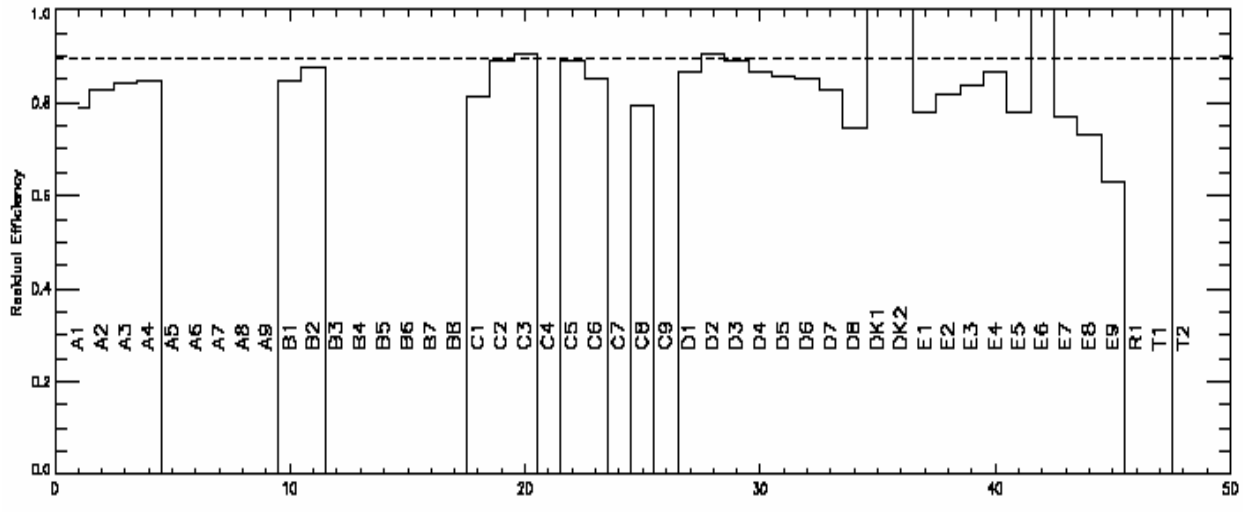

Figure 3: Ratio between measured and expected absorbed power onto the bolometers for photometer 520-μm channel, taken from a comparison between the absorbed power with the CBB at 6.4 and 13.168 K.

The modelled instrument transmissions (not including the detector feedhorn efficiency) are 0.37, 0.44, 0.48 for the 250, 360 and 520-μm bands. To estimate the true transmission efficiency we can multiply the expected transmission by the calculated ratio of measured to expected (shown by the dotted line in Fig. 3). The calculated ratios are ~ 0.9, 0.77, 0.85 respectively for 250, 360 and 520 μm, giving overall transmission values of 0.33, 0.34 and 0.41. These are the maximum figures and as we see from the plots there are some gradients across the array. The requirement of 0.27 is met in all cases.

The same procedure as used for the photometer was carried out on the spectrometer. Additionally, we assume that only 50% of the power is seen as the SMEC was always set away from the zero path difference (ZPD) position. In a similar manner to the photometer we can estimate the total transmission of the spectrometer to be about 0.17. To evaluate the transmission efficiency the CBB was set to 6.4 K and 15.5 K and the increase absorbed power calculated from a comparison of load curves. The resulting efficiency is greater than unity for almost all detectors. A possible explanation, currently under investigation, is that the feedhorn efficiency is high even for the higher order modes, resulting in a large background, especially for the SLW array. This is apparent from spectral measurements of the passband expressed as the ratio of the power observed to that expected from a single moded instrument. Further modelling and experimentation is planned in order to arrive at a better understanding of the spectral characteristics of the FTS arrays.

5. OPTICAL TESTING

5.1 Spectral passbands

The photometer and spectrometer passband specifications are listed in Table 2. For the photometer the spectral passband was measured using the external FTS and the hot black body source. All of the photometer passbands have been found to be in spec, except for some small deviations in the case of the 520 μm array for which most pixels have a short wavelength cutoff slightly lower than the specification (with negligible scientific impact).

For the spectrometer, the sources used to determine the band edges were the spectrometer calibrator (SCAL) and the cold black body source. Both the SSW and SLW arrays meet requirements although the current measurements on SW array have large uncertainties which need to be reduced by further measurements.

	Photometer band			Spectrometer band	
	250 μm	363 μm	517 μm	SSW band	SLW band
λ_{Lower} (μm)	208.3 +/- 2.1	306.0 +/- 3.1	430.8 +/- 4.3	188 - 192	297 - 303
λ_{Upper} (μm)	291.7 +/- 8.5	420.0 +/- 12.3	603.2 +/- 17.6	321 - 329	666 - 683
$\lambda_o/\Delta\lambda$	3.00 +/- 0.39	3.18 +/- 0.45	3.00 +/- 0.39		

Table 2: Specifications for the photometer and spectrometer band edges.

5.2 Beam profiles and field of view

The pixel positions in the field of view (FOV) were measured via peak-up tests in which a point source viewed through the telescope simulator was stepped across a pixel in a cross pattern. A similar technique was used to determine the beam profile in two dimensions where instead of a cross pattern, a square raster was used. The source used was either the hot blackbody or the laser.

The co-alignment of the spectrometer arrays has been found to be within predictions from the optical model. It has not yet been possible to fully verify the photometer array co-alignment due to a fault with one of the dichroics which is viewed in reflection by the 320 μm array. This problem has now been corrected, and early indications from the current cooldown data indicate that the arrays are co-aligned within the specification

The photometer beam profile measurements have not yet been fully analysed. During the CQM tests, a FWHM of 30 ± 5" was measured for the 520-μm array at 432 μm, equivalent to 35 ± 6" at 520 μm. This is close to the expected value of 36". The uncertainty will be reduced by the analysis of data already acquired during FM testing, and similar measurements will be carried out of the beam profiles for the two other channels. The beam profiles for the spectrometer bands are expected to be wavelength dependent due to the significant multi-moding of the feedhorns. This has not been modelled in detail, and the beam profiles will need to be evaluated from instrument-level measurements, some of which have already been made. The spectrometer SSW FWHM was found to be 16 ± 2" 250 μm. The SLW FWHM was found to be > 40" below ~ 310 μm and < 30" above 500 μm. Further characterisation of this wavelength dependence will be made during the current and future cooldown campaigns.

6. INTERNAL CALIBRATOR PERFORMANCE

The performance of the photometer calibrator has been verified in terms of electrical power dissipation, radiant power measured at the detectors, and time response. A standard PCal flash sequence has been established and is used regularly during all tests as a check on detector responsivity and general diagnostic of the system. The optimum operating levels and sequence for flight will be determined during ground calibration. PCal is centrally located at a pupil in the BSM, and so should illuminate the arrays uniformly (although it is not required to do so). Tests indicate that the illumination is actually brightest towards one of the long edges of the arrays.

Tests have been carried out on the flight model to evaluate the SCal thermal performance, time constant, achieved equilibrium temperature vs. applied power, and the ability to null the background spectrum. For the thermal tests, a variety of constant current levels were applied to both of the SCal emitters, and the resulting warm-up curves were recorded. From these stabilisation times were determined, and were typically ~ one hour. The analysis of this data has allowed a refinement of the warm up procedure which will reduce stabilisation times to around 15 minutes (to be verified experimentally in future tests).

At each SCal setting tested, once thermal stability had been achieved, a load curve was taken. Analysis is in progress to determine the SCal power output and uniformity. The operating stability has been found to be within the required ± 2

mK over several separate periods of eight hours. The stability requirement has been met during lifetime tests at unit level.

A nulling test was performed in which the SCal source temperature was set and the cold blackbody temperature (filling the other port) was varied. This was done for both the 2% and 4% SCal sources. For each detector, the ZPD position height was measured as a function of the cold blackbody temperature. The temperature at which the central maximum reduces to zero was then derived from the fit over the range of temperatures. The nulling temperatures found are in good agreement with the photometric model of the SCal and cold blackbody system.

More details of the evaluation of PCal and SCal are given in Hargrave *et al*.[7].

7. BEAM STEERING MECHANISM PERFORMANCE

A set of FOV scans was used to characterise the BSM optically and also to determine its movement range. From these scans, the movement range in the chop axis was found to be 378" (± 189"), which is better than the requirement. Due to the pixel layout, and the more limited movement range, the jiggle axis is much more difficult to characterise using the FOV scanning method. The jiggle axis scans showed that the BSM reached the centre of pixels on three adjacent rows on the PMW array with a pixel separation of about 50" apart; hence the 30" range requirement is exceeded. A preliminary calibration of the BSM shows that 1" corresponds to 185 position units in the chop axis. As the BSM is commandable to a single position unit, the ability to set a minimum step of 2" in operations is also met.

The BSM chopping mode requires a closed loop PID control and the control system parameters need to be tuned for the control electronics. As the BSM was used with the instrument electronics for the first time during instrument level testing, this was the first opportunity to tune the BSM system, and following some refinements to the procedure, tuning has been achieved successfully. Tests have been carried out at the nominal chop frequency of 2 Hz, but the extended range (up to 5 Hz) has yet to be verified. Sub-arcsecond stability has been demonstrated at a hold position but not yet during chopping as the lack of tuning means that there is an overshoot at each commanded position followed by a settling time. If this overshoot time is ignored the stability within the remaining time per cycle is less than 0.1". The settling time specification of 20 ms has not yet been met with the best figure yet achieved being 28 ms. It is expected that this will be met following fine tuning during the next campaign.

8. SPECTROMETER PERFORMANCE

The performance of the spectrometer system is reported in detail by Spencer *et al.*[8] and Naylor *et al.*[9] Tests to date have been carried out on a flight-like spectrometer mechanism. The maximum resolution of the spectrometer was derived from measurements in which the far infrared laser was used to provide an unresolved spectral line. A sinc function was fit to the measured spectrum of the laser line and the resolution was determined by the full width at half maximum of the fit. The results show that the resolution requirement of 0.4 cm^{-1} has been met. The goal of 0.04 cm^{-1} has not yet been demonstrated due to the less-than-maximum SMEC mechanical travel that has so far been available during testing, and is expected to be met with the flight spectrometer mechanism. For the low-resolution spectrophotometry mode of the FTS, it was found that the requirement of 1 cm^{-1} can be met (although it is foreseen that in flight a value of 1 cm^{-1} will be adopted as optimum for most scientific purposes).

Fringe contrast and passbands are also close to expectations and the ability to null the interferogram central maximum using SCal has been verified. key requirements are met. Further detailed characterisation of the FTS will be carried out when the flight model mechanism is installed.

9. CONCLUSIONS AND PLANS FOR FUTURE TEST CAMPAIGNS

Ground testing of the SPIRE flight instrument is underway and results so far have shown that the instrument is performing very well and in general meets not only its requirements but also most of its performance goals. Although several test campaigns have taken place, the flight spectrometer mechanism and warm electronics units are still to be installed. Various aspects of the instrument performance are still to be verified – additional testing, together with optimisation of some instrument parameters and detailed instrument calibration will be carried out in subsequent cooldown campaigns.

REFERENCES

1. M. Griffin, A. Abergel, P. Ade, P. André, J-PBaluteau, J. Bock, A. Franceschini, W. Gear, J. Glenn, D. Griffin, K. King, E. Lellouch, D. Naylor, G. Olofsson, I. Perez-Fournon, M. Rowan-Robinson, P. Saraceno, E. Sawyer, A. Smith, B. Swinyard, L. Vigroux, and G. Wright, *Herschel-SPIRE: Design, Performance, and Scientific Capabilities*, in *Space Telescopes and Instrumentation I: Optical, Infrared, and Millimeter*, Orlando, 24-31 May 2006, *Proc. SPIE* 6265 (this volume).
2. G. Pilbratt, *Herschel Mission: status and observing opportunities*, in *Space Telescopes and Instrumentation I: Optical, Infrared, and Millimeter*, Orlando, 24-31 May 2006, *Proc. SPIE* 6265 (this volume).
3. T. Lim, B. Swinyard, A. Aramburu, J. Bock, M. Ferlet, D., Griffin, M. Griffin, P. Hargrave, K. King, S. Leeks, D. Naylor, S. Ronayette, E. Sawyer, B. Schulz, S. Sidher, L. Spencer, D. Smith, and A. Woodcraft, *First Results From Herschel-SPIRE Performance Tests, Proc. SPIE* 5487, 460, 2004.
4. P.A. Collins, D.L. Smith, M. Ferlet, T. Grundy, M. Harman, M.J. Griffin, P.A.R. Ade, and B.M. Swinyard, *Ground calibration facility for Herschel-SPIRE*, *Proc. SPIE* 4850, 628, 2003.
5. L. Spencer, D. Naylor, B. Swinyard, A. Abreu Aramburu, T. Fulton, T. Lim, S. Ronayette, and I. Schofield, *A Fourier transform spectrometer for ground testing of the Herschel/SPIRE instrument*, Proc. SPIE 5487, 501, 2004.
6. R.V. Sudiwala, M.J. Griffin, and A.L. Woodcraft, "Thermal modelling and characterisation of semiconductor bolometers", *Int. Journal of Infrared and Mm Waves*, 23, 545, 2002.
7. P. Hargrave, T. J. Waskett, T. L. Lim, and B.M. Swinyard, *Performance of flight-model on-board calibration sources on Herschel-SPIRE*, in *Millimeter and Submillimeter Detectors and Instrumentation for Astronomy III,* , Orlando, 27-31 May 2006, *Proc. SPIE* 6275.
8. L.D. Spencer, D.A. Naylor, and B.M Swinyard, *A comparison of the theoretical and measured performance of the Herschel/SPIRE imaging Fourier Transform Spectrometer*, in *Space Telescopes and Instrumentation I: Optical, Infrared, and Millimeter*, Orlando, 24-31 May 2006, *Proc. SPIE* 6265 (this volume).
9. D.A. Naylor, J-P. Baluteau, P. Davis-Imhof, M.J. Ferlet, T.R. Fulton, and B.M. Swinyard, *Performance evaluation of the Herschel/SPIRE imaging Fourier Transform Spectrometer*, in *Space Telescopes and Instrumentation I: Optical, Infrared, and Millimeter*, Orlando, 24-31 May 2006, *Proc. SPIE* 6265 (this volume).